Langmuir

ARTICLE

pubs.acs.org/Langmuir

Interaction Between Zwitterionic and Anionic Surfactants: Spontaneous Formation of Zwitanionic Vesicles

Sampad Ghosh, Dibyendu Khatua, and Joykrishna Dey*

Department of Chemistry, Indian Institute of Technology, Kharagpur-721 302, India

Supporting Information

ABSTRACT: The physicochemical properties, such as critical micelle concentration (cmc), surface tension at cmc (γ_{cmc}), and surface activity parameters of the mixtures of a new amino acid-based zwitterionic surfactant, *N*-(*n*-dodecyl-2-aminoethanoyl)-glycine (C_{12}Gly) and an anionic surfactant, sodium dodecyl sulfate (SDS) at different molar fractions, X_1 (= [C_{12}Gly]/([C_{12}Gly] + [SDS])) of C_{12}Gly were studied. A synergistic interaction was observed between the surfactants in mixtures of different X_1. The self-organization of the mixtures at different molar fractions, concentrations, and pH was investigated. Fluorescence depolarization studies in combination with dynamic light scattering, and transmission electron microscopic and confocal fluorescence microscopic images suggested the formation of bilayer vesicles in dilute solutions of SDS rich mixtures with $X_1 \leq 0.17$ in the pH range 7.0 to 9.0. However, the electronic micrographs showed structures with fingerprint-like texture in moderately dilute to concentrated C_{12}Gly/SDS mixture at $X_1 = 0.50$. The vesicles were observed to transform into small micelles upon lowering the solution pH and upon increase of total surfactant concentration in mixtures with $X_1 \leq 0.17$. However, decrease of SDS content transformed vesicles into wormlike micelles. The structural transitions were correlated with bulk viscosity of the binary mixtures.

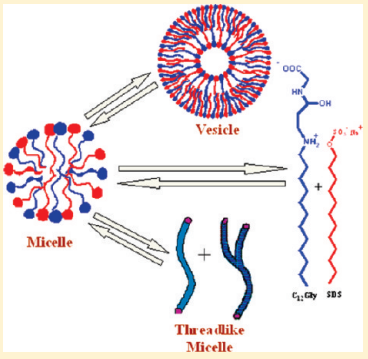

1. INTRODUCTION

It is well-known that many biological or synthetic-based self-assemblies and interfaces consist of surfactant mixtures. Since self-assemblies composed of mixed surfactants occur in biological fluids, mixed surfactants are very often preferred in industrial preparations and pharmaceutical and medicinal formulations for the purpose of solubilization, suspension, dispersion etc.[1−3] Thus, for most practical applications mixed surfactants are used rather than single surfactants. Typical detergent formulations also consist of two or more types of surfactants, the major component of which is usually a conventional pH-insensitive surfactant. However, often small amounts of pH-sensitive surfactants are added to boost detergent performance. In most cases, the mixed system results in enhanced interfacial properties, such as lower critical micelle concentration (cmc) and higher surface activity relative to the individual surfactants. This is known as *synergism*. There are many reports in the literature on the studies of different combinations of mixed surfactant system viz. cationic/cationic,[4] nonionic/nonionic,[4,5] anionic/nonionic,[6,7] etc. Solubilization behavior of different compounds in the mixed micellar solution has been observed to be better than individual surfactant micelles.[8−10] It is believed that detergency is related to micellar stability and that the addition of surfactant of opposite charge is one of the factors enhancing micellar stability. However, micellar stability is directly correlated to Coulombic repulsions. The addition of oppositely charged surfactant diminishes the surface charge density of the mixed micelles and hence minimizes the charge repulsion between micelles. In recent years, mixed surfactant systems containing anionic and cationic surfactants have attracted tremendous attention because they exhibit spontaneous formation of stable unilamellar vesicles in dilute solutions.[11,12] Kaler et al. were the first to report this in a study on three different cationic/anionic surfactant systems.[11] Since then, numerous other cationic/anionic systems have been investigated.[13−16] These have been summarized in many reviews.[17]

Although a lot of effort has been devoted to understanding the behavior of cationic/anionic systems, only a few studies on the zwitterionic/anionic (zwitanionic) systems have been reported.[18] These studies have revealed that zwitterionic surfactants often have strong interaction with anionic surfactants. However, in contrast to cationic/anionic systems, the attraction forces between the two kinds of surfactants in the zwitanionic systems are expected to be weak. McLachlan et al.[19] determined cmc values for the zwitanionic systems of *N*-dodecyl-*N*,*N*-dimethyl-3-ammonio-1-propanesulfonate (ZW3-12)/sodium dodecyl sulfate (SDS), *N*-dodecyl-*N*,*N*-(dimethylammonio)-butyrate (DDMAB)/SDS, *N*-octyl-*N*,*N*-dimethyl-3-ammonio-1-propanesulfonate (ZW3-08)/sodium octyl sulfate (SOS). Evidence of strong interactions between zwitterionic and anionic surfactants in each of the zwitanionic systems has been reported. The ZW3-08/SOS and DDMAB/SDS mixed systems were observed to behave synergistically at all mole fractions studied while the ZW3-12/SDS mixed system exhibited synergistic behavior above mole fractions of 0.30 only. Li et al.[20] investigated

Received: October 5, 2010
Revised: March 3, 2011
Published: April 04, 2011

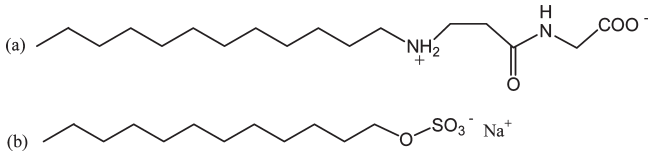

Figure 1. Chemical structures of (a) C_{12}Gly and (b) SDS surfactants.

the interaction between sodium dodecyl sulfonate (C12AS), and three zwitterionic surfactants (alkyldimethylammoniopropane sulfonates of varying alkyl chain length, abbreviated as C12DPAS, C10DPAS, and C8DPAS). They observed that the strongest interaction occurred between C12AS and C12DPAS, while the weakest interactions were observed between C12AS and C8DPAS. According to the authors, the electrostatic attraction between the $N^+(CH_3)_2$ group in the zwitterionic surfactant and the SO_3^- group in C12AS is responsible for the synergistic effect. In the mixture formed by tetradecyldimethylamine oxide (TDMAO) and calcium dodecyl sulfate (CDS) containing an excess of TDMAO at constant 100 mM of total amphiphile concentration, Hoffmann et al.[21] detected a birefringent lamellar phase composed of densely packed onion-like vesicles. Weiss et al.[22] studied the dynamics of spontaneous vesicle formation in mixtures of TDMAO and lithium perfluorooctanoate (LiPFO) and TDMAO and lithium perfluorooctane sulfonate (LiPFS). A disk-like micelle was detected as the metastable state in the micelle-to-vesicle transition. Denkov and co-workers[23] have reported synergistic sphere-to-rod micelle transition in mixed systems of SDS and cocaamidopropyl betaine, a zwitterionic surfactant. There are also a few reports which have briefly addressed vesicle stability in zwitanionic surfactant systems.[24,25]

In the work presented here, we have performed a study of the general behavior of zwitanionic surfactant system with *N*-(*n*-dodecyl-2-aminoethanoyl)-glycine (C_{12}Gly) (see Figure 1 for structures) as zwitterionic surfactant and SDS as anionic surfactant. The former amphiphile is a pH-sensitive surfactant and is expected to have performance-boosting properties, such as low potential for skin and eye irritation and good foaming characteristics. Accordingly, our aim is to study the interaction between the surfactants with our main interest being the extent of vesicle formation in such mixtures. Since C_{12}Gly is pH-sensitive, it may find applications in controlled drug release, targeted gene delivery, and fabrication of nanomaterials. In order to evaluate these, we have studied the aggregation behavior of the C_{12}Gly/SDS mixtures in water at different mixing ratios, concentration, and pH. The C_{12}Gly/SDS mixed system has been characterized by a number of techniques, including surface tension (ST), fluorescence, dynamic light scattering (DLS), and transmission electron microscopy (TEM).

2. EXPERIMENTAL SECTION

2.1. Materials. The amphiphile C_{12}Gly was synthesized and purified according to the procedure reported in our earlier papers.[26−28] ^{1}H, ^{13}C NMR, and IR spectra were used for chemical identification of the compound. The fluorescence probe 1,6-diphenyl-1,3,5-hexatriene (DPH), 5(6)-carboxyfluorescein (CF), cholesterol (Chol), and SDS were procured from Aldrich and were purified by recrystallization from acetone-ethanol mixture. Doubly distilled water was used for solution preparation.

2.2. Methods. *General Instrumentation.* The ^{1}H NMR spectra were recorded on a Bruker 200 MHz spectrometer. UV−vis spectra were recorded on a Shimadzu (model 1601) spectrophotometer. Bulk viscosity of surfactant solutions were measured with a Vibro viscometer (Model: SV-1A, A&D,Tokyo, Japan) instrument. Thermo Orion model 710A+ digital pH meter was used to measure the pH of the solutions. Temperature was controlled using a Thermo Neslab RTE −7 circulating bath.

Solution Preparation. The surfactants were mixed in a volumetric flask in desired molar fractions of C_{12}Gly ($X_1 = [C_{12}Gly]/([C_{12}Gly] + [SDS])$) using appropriate volume of respective stock solution (100 mM) in methanol. The solvent was dried in water bath. This ensured ion-pair formation between C_{12}Gly and SDS surfactants as reported for C_{12}Ala/SDS system.[32] Aqueous solutions of known concentrations were obtained by adding appropriate volumes of buffer solution of desired pH to the dry mixture. The DPH concentration was adjusted to 1.0 μM by addition of an appropriate amount of the stock solution (1.0 mM) made in 20% (v/v) methanol−water mixture.

Surface Tension Measurements. The surface tension (γ) of the surfactant solutions were measured using Du Nuöy ring detachment method with an automated surface tensiometer (3S, GBX, France) at ∼30 °C. The instrument was calibrated through loading proper weight (for 600 mg the γ shows 49 mN m^{-1}) and checked by measuring the surface tension of distilled water before each experiment. Aliquot of the stock solution in distilled water was transferred to a beaker containing known volume of water. The mixture was magnetically stirred for 30 s following each addition of aliquot and allowed to stand for about 3 min at room temperature (∼30 °C) to achieve equilibrium before surface tension was measured. For each concentration, three measurements for γ were performed and their mean was taken as the value of the equilibrium surface tension.

Fluorescence Measurements. Steady-state fluorescence spectra of DPH were measured with a Perkin-Elmer LS-55 luminescence spectrometer equipped with filter polarizers that uses the L-format configuration. The excitation slit with bandpass of 2.5 nm and the emission slit with bandpass between 2.5 and 10 nm were used for the measurements. The samples containing DPH were excited at 350 nm and the emission intensity was measured in the range 360−560 nm. All spectra were blank subtracted. For anisotropy measurements, the fluorescence intensity was monitored at 450 nm and a 430 nm cutoff filter was placed in the emission beam to eliminate the effects of scattered radiation. An average of six measurements were always recorded. A quartz cell of 10-mm path length was used for all fluorescence measurements.

Dynamic Light Scattering (DLS) Measurements. The DLS measurements were carried out by a home-built spectrometer the details of which are available elsewhere.[29] A 15-mW He−Ne laser (λ_o = 633 nm) was used for the measurements. The scattering radiation was measured at 90° to the incident beam. For some measurements, we also used Zetasizer Nano ZS (Malvem Instrument Lab, Malvern, U.K.) The intensity autocorrelation functions were analyzed using method of cumulant.[30]

Transmission Electron Microscopic (TEM) Measurements. For TEM micrographs, 5 μL of solution was placed on a 400 mesh size carbon-coated copper grid allowed to adsorb for 30 s. Excess liquid was wicked off by use of a piece of filter paper, air-dried, and then negatively stained with freshly prepared 1.0% aqueous uranyl acetate. The specimens were kept in desiccators until before use. The specimens were examined under a transmission electron microscope (JEOL-JEM 2100, Japan) operating at an accelerating voltage of 200 kV at room temperature (298 K).

Fluorescence Microscopic Measurements. Optical microscopic measurements of dye (CF) trapped vesicles were performed using a FV 1000 Olympus Confocal Microscope equipped with a laser scanning module (LSM) microscope and a PLAPON 60X oil immersion objectives with numerical aperture (NA) of 1.42. For CF trapped vesicles 488 nm laser was used and the filter was 520 nm. For entrapment of dye into the vesicles 5 mM dye, 3 mM C_{12}Gly/SDS mixture, and 10-mol % Chol

dx.doi.org/10.1021/la1040147 |*Langmuir* 2011, 27, 5184–5192

were taken in methanol, mixed, and dried thoroughly by rotary evaporation in a round-bottom flask. The thin film of the mixture thus obtained was soaked with small volume of phosphate buffer (pH 7.4, 150 mM NaCl) overnight, vortexed, and then diluted to the desired volume to obtain 3 mM vesicular solution. Excess dye was removed by dialysis using an ultrafiltration cellulose acetate membrane (pore size 10 kDa MWCO, Diam 16 mm) bag for about 4−6 h. An aliquot of the undiluted vesicle solution was pipetted into the microscopic glass slide (Riviera, 25.4 × 76.2 mm), which was then sealed with a coverslip and left for a few minutes before analysis. Images were projected and analyzed using FV10-ASW 1.6 Viewer software.

3. RESULTS AND DISCUSSION

3.1. Solubility Studies. The solubility of C_{12}Gly in water (pH = 6.5) was found to be very poor (ca. 0.6 mM) at room temperature, indicating zwitterionic nature of the amphiphile. The solubility, however, increases with the rise of temperature and solution pH. The amphiphile becomes readily soluble in water in alkaline pH (>12) at which it exits in the anionic form. Despite zwitterionic character, a significant solubility of the amphiphile could be achieved in phosphate buffer (pH 7.4) due to salting in phenomenon. Therefore, the interaction studies with SDS were done in phosphate buffer at pH 7.4. For the interaction studies, first, stock solutions (100 mM) of individual surfactants were made in methanol. Aliquots of each solution were mixed in 5-mL volumetric flasks to obtain mixtures containing varying total concentrations at a fixed molar fraction, X_1 or of varying X_1 at a fixed total concentration. The solvent was removed using a hot water bath and an appropriate volume of phosphate buffer was added to prepare aqueous solutions. The pH of the aqueous C_{12}Gly/SDS mixtures did not change significantly. The C_{12}Gly/SDS mixtures with $X_1 \leq 0.5$ remained soluble in water at all concentrations. However, mixtures with X_1 = 0.6 resulted in isotropic solutions only at concentrations greater than 3.5 mM. Therefore, all studies on C_{12}Gly/SDS mixtures with X_1 = 0.6 were carried out at a total concentration greater than 4.0 mM. It should be noted that the mixtures with X_1 > 0.6 did not produce isotropic solution in the concentration range (0−30 mM) studied here and therefore were not investigated. When the total concentration was raised above 3.5 mM, initially an isotropic solution was obtained, which either turned cloudy or a fibrous precipitate (depending upon concentration and molar fraction) appeared after a while. ^{1}H NMR spectrum (not shown) of the precipitate confirmed pure C_{12}Gly. The molar fraction being higher the concentration of C_{12}Gly is much higher compared to SDS ([SDS] < cmc) at X_1 > 0.6 and as a result, remains insoluble even at a total concentration as high as 30 mM.

3.2. Surface Properties of the Pure Surfactants and their Mixtures. The cmc values and other physicochemical properties of the pure as well as binary surfactant mixtures (C_{12}Gly/SDS) were determined by ST measurements. The ST versus log C plots have been depicted in Figure S1 of "Supporting Information". The concentration corresponding to the break point of the surface tension (γ) versus log C plot was taken as the cmc value. These plots showed that the γ_{cmc} values for the surfactant mixtures were much lower than that of pure SDS (X_1 = 0) or C_{12}Gly (X_1 = 1) surfactants. The cmc of the C_{12}Gly/SDS mixtures of different compositions (X_1 = 0.17 to 0.50) was obtained from ST plots. The cmc values along with the surface activity, f_1, and X_{1m} data have been listed in Table 1. The data in

Table 1. Values of cmc, γ_{cmc}, pC_{20}, f_1, X_{1m}, and β parameter for various compositions (X_1) of C_{12}Gly/SDS (pH 7.4) mixtures at 30 °C

X_1	cmc (±0.10) (mM)	γ_{cmc} (mN/m)	pC_{20}	f_1	X_{1m}	β
1.00	0.64	43.0	3.84			
0.50	0.25	21.3	4.74	0.317	0.616	−7.79 ± 0.31
0.33	0.32	21.0	4.67	0.284	0.583	−7.24 ± 0.39
0.25	0.37	20.9	4.61	0.256	0.564	−7.16 ± 0.36
0.17	0.49	20.8	4.63	0.237	0.538	−6.75 ± 0.36
0.00	7.62	37.1	2.84			

Table 1 show that the cmc value decreases with the increase of X_1 value (i.e., decrease of SDS content in the mixture). The pC_{20} (negative logarithm of surfactant concentration required to reduce the surface tension of water by 20 units at the temperature of measurement) values of the mixed surfactant systems are observed to be much higher than that of pure SDS. It is also observed that the C_{12}Gly/SDS mixtures have much lower γ_{cmc} value as compared to pure SDS. These suggest that the surfactant mixtures behave as better surface-active agents in comparison to pure SDS. Such synergistic affects have been reported for many cationic/anionic systems.[17] In the case of C_{12}Gly/SDS system, the synergism could be attributed to strong electrostatic interaction between the $>NH_2^+$ group of C_{12}Gly and SO_3^- group of SDS surfactants to form a pseudodouble chain carboxylate surfactant. The stronger hydrophobic interaction among hydrocarbon chains of the pseudodouble chain surfactant thus formed lowers the cmc value as well as the air/water interfacial tension (γ_{cmc}).

3.3. Surfactant−Surfactant Interactions. It has been shown that the interaction parameter β obtained from regular solution theory[31] is useful in understanding the nature and strength of interactions between two nonhomologus surfactants in solution. The β values explain the interaction between headgroups of the two surfactants. It does not include the interaction between hydrocarbon chains of the surfactants when the chain lengths are different. Classically, the interaction parameter β is determined by measuring cmc of the corresponding surfactant mixtures. The interaction between C_{12}Gly and SDS surfactants in the mixed aggregate was measured by calculating β from equations derived using Rubingh's theory of nonideal mixing.[32] Nonideality can be analyzed by regular solution theory[31,33] according to which the cmc's of surfactant mixtures (C_{12}) are given by the following:

$$C = X_{1m} f_1 \cdot C_1 = X_1 \cdot C_{12} \quad (1)$$

where C_{12} and C_1 are the cmc's of the binary mixture and surfactant 1 (C_{12}Gly), respectively, C and X_1 are the concentration and molar fraction of surfactant 1 in solution, respectively, X_{1m} is the molar fraction of surfactant 1 in the mixed micelle, and f_1 is the activity coefficient which is given by eq 2

$$\ln f_1 = \beta(1 - X_{1m})^2 \quad (2)$$

Since $f_1 = [C_{12}(1 - X_1)/C_2(1 - X_{1m})]$, eq 2 can be rewritten as follows:

$$\frac{X_{1m}^2 \ln(C_{12}X_1/C_1X_{1m})}{(1 - X_{1m})^2 \ln\{C_{12}(1 - X_1)/C_2(1 - X_{1m})\}} = 1 \quad (3)$$

where C_2 is the cmc of surfactant 2 (SDS). X_{1m} can be calculated solving eq 3 iteratively. The interaction parameter β was

evaluated from the X_{1m} value thus obtained and experimentally determined C_{12} (i.e., cmc of the mixed system) value using the following equation:[31,33]

$$\beta = \frac{\ln(C_{12}X_1/C_1X_{1m})}{(1-X_{1m})^2} \quad (4)$$

It should be noted that β is a dimensionless parameter that can be experimentally determined from the cmc values according to eq 4. The interaction parameter β thus obtained for different molar fraction (X_1) of C_{12}Gly have been listed in Table 1. From the data in Table 1, it can be found that the β values for all compositions of binary mixtures are negative, which suggests that the interaction between C_{12}Gly and SDS surfactants is more attractive in the mixed micelle than the self-interaction of the surfactants before mixing. According to regular solution theory,[19,20,34] the β parameter values should be independent of composition. Indeed, for mixtures with $X_1 = 0.25$ and 0.33, within the experimental error limit, the β parameter values are equal. However, a slightly lower and higher value of β parameter for mixtures with $X_1 = 0.17$ and $X_1 = 0.50$, respectively might be due to the formation of self-assemblies other than mixed micelles. This has been discussed below. The synergistic interaction is supported by the fact that the $|\beta|$ value is greater than $|\ln(C_1/C_2)|$ (~2.5). Similar behavior has also been reported for other zwitterionic/anionic systems.[34] However, it should be noted that unlike other zwitterionic/anionic systems, the $|\beta|$ value for the C_{12}Gly/SDS system is higher, indicating stronger interaction. That the mixing is nonideal is shown by the activity coefficient (f_1) values that are much less than 1.0. The data in Table 1 also show that irrespective of the solution composition the molar fraction of C_{12}Gly in the mixed micelle (X_{1m}) is ca. 0.5. This, as discussed above, supports the formation of 1:1 complex which produce mixed micelles at a concentration above the cmc value.

According to solution theory of Motomura and co-workers,[35] the micelle behaves thermodynamically like a macroscopic bulk phase in which azeotropy is closely related to the interaction between constituent molecules in the mixture. The azeotropic behavior of the micellar system is determined by the molecular interaction between the surfactants. It is well-known that negative azeotropy takes place if the molecular interaction between components is attractive and pure components have similar vapor pressure values. Therefore, we can conclude that the C_{12}Gly/SDS mixtures will exhibit negative azeotropy as the interaction between the surfactants is attractive in nature. Such behavior has also been shown by copper dodecyl sulfate-sodium tetradecyl sulfate, and tetraoxyethylene octyl ether-sodium dodecyl sulfate systems.[36]

3.4. Self-Assembly Formation. Earlier work from this laboratory has suggested that morphology of surfactant aggregates can be predicted based on the results of microenvironment study by fluorescence probe technique.[37] In fact, the steady-state fluorescence anisotropy (r) of DPH probe is often used to predict the type of aggregates formed in aqueous solutions of various surfactants. The DPH molecule is solubilized in the hydrocarbon region of surfactant aggregates. Consequently, its rotational diffusion and hence fluorescence anisotropy is influenced by the fluidity of the microenvironment of the aggregates. It has been shown that for bilayer aggregates, usually the fluorescence anisotropy of DPH is high ($r > 0.14$)[27] and for spherical or rod-like micelles, the r-value is lower ($r < 0.14$).[37,38] This is because the hydrocarbon chains are tightly packed in bilayer aggregates

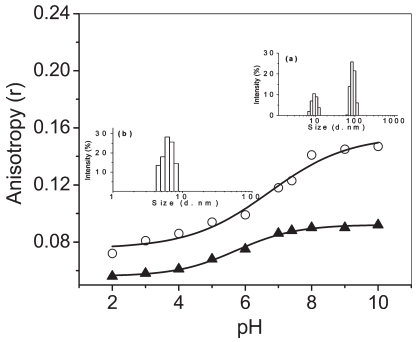

Figure 2. Plots of fluorescence anisotropy (r) of DPH in 3 mM C_{12}Gly/SDS mixture as a function of pH at 30 °C for molar fractions (○) 0.17, (▲) 0.5; inset: size distributions of aggregates in 3 mM C_{12}Gly/SDS mixtures at (a) pH 7.4, and (b) pH 3.0.

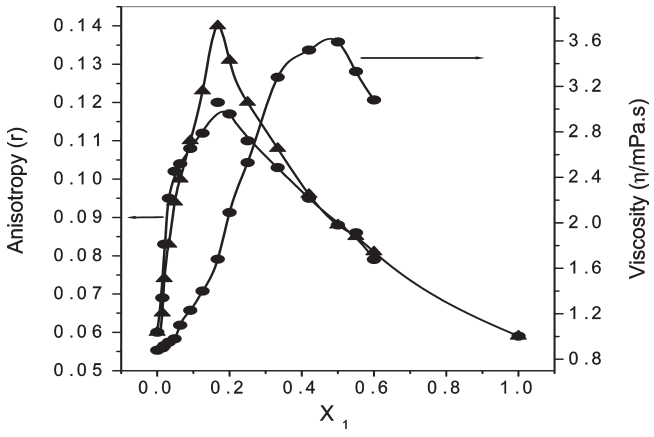

Figure 3. Variation of solution viscosity (η) pH 7.4 and fluorescence anisotropy (r) of DPH as a function of molar fraction (X_1) of C_{12}Gly surfactant in 3 mM C_{12}Gly/SDS mixtures at 30 °C: (●) pH 7.4 and (▲) pH 9.0.

and therefore the microenvironment is more rigid which means less fluid. However, in normal micelles, the hydrocarbon chains of the surfactants are less tightly packed and hence the microenvironment is more fluid like hydrocarbon solvents. Therefore, r-value can be used as an index of microviscosity (more appropriately microfluidity) of the local environment of the DPH molecule. Usually, bilayer aggregates have higher microviscosity compared to micellar aggregates.[37] Therefore, fluorescence studies using DPH were performed with various compositions and different concentrations of the C_{12}Gly/SDS system.

Effect of Solution pH. Since C_{12}Gly is amphoteric in nature, its self-assembly behavior in the presence of SDS should be dependent on solution pH. This is shown by the variation of r-value of the DPH probe with pH (Figure 2). It is observed that C_{12}Gly/SDS mixture ($X_1 = 0.17$ and 0.5) has highest r-value at pH 9.0, which decreases as acidity of the solution is increased. The higher r-value at pH 9.0 is indicative of the formation of bilayer aggregates. The existence of large aggregates in pH 9.0 is confirmed by the mean hydrodynamic diameter (~100 nm) of the aggregates as shown by the size distribution histogram (inset of Figure 2). The lowering of r-value can be attributed to transformation of bilayer aggregates into either small spherical or rod-like micelles. This is indicated by the particle size (~5 nm) in pH 3 (inset of Figure 2). Since DLS technique cannot

dx.doi.org/10.1021/la1040147 |*Langmuir* 2011, 27, 5184–5192

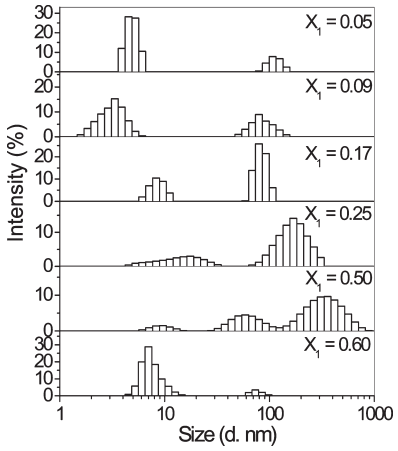

Figure 4. Size distribution histograms of the aggregates formed in 3 mM C_{12}Gly/SDS mixtures (pH 7.4) of different compositions at 30 °C.

distinguish between different shapes of particles, it is not possible to comment on whether the small particles are normal micelles or rod-like micelles. The inflection point of both plots in Figure 2 is around pH 6.0 and corresponds to pK_a value of the −COOH group of C_{12}Gly. The protonation of the $-COO^-$ group makes the negatively charged surfactant (1:1 complex) uncharged and hence cause precipitation at pH < 3.0. Since the vesicle phase exists in pH > 7, subsequent studies were performed at pH 7.4 and 9.0.

Effect of Composition. The variation of *r*-value with molar fraction (X_1) of C_{12}Gly in pH 7.4 and 9.0 has been shown by the plots in Figure 3. The feature of both plots shows that *r*-value of the pure C_{12}Gly (X_1 = 1.0) is very low and corresponds to normal micelles, but upon addition of SDS the *r*-value slowly increases reaching maximum at X_1 = 0.17. Further addition of SDS, however, decreases *r*-value which reaches minimum at X_1 = 0 corresponding to pure SDS solution. The relatively high *r*-value of DPH in solution at X_1 = 0.17 is indicative of the existence of bilayer aggregates, which transform into micelles (spherical or rod-like) as the SDS content is increased or decreased in the mixture. In bilayer aggregates, the hydrocarbon chains are tightly packed making the microenvironment very rigid and less polar. The transformation of bilayer structures to normal micelles makes the packing of the hydrocarbon chains less tight and thus allows more water molecules to penetrate into the interfacial region resulting in an increase of micropolarity and microfluidity.

It is interesting to note that there is an increase in solution viscosity, η (see Figure 3) of the mixtures with the decrease of SDS content reaching maximum at X_1 = 0.50. However, the solution viscosity dropped down again in mixture with X_1 = 0.6. Thus, it is clearly evident that substantial structural changes take place in the mixtures upon changing the mixing ratio. Similar behavior has also been reported for TDMAO/LiPFO system.[25] Such a viscosity increase must be due to the formation of wormlike micelles. Alternatively, this could also be due to formation of disk-like micelles or lamellar sheets. The possibility of formation of lamellar sheets or disk-like micelles, however, can be ruled out based on the relatively lower *r*-values in mixtures of X_1 > 0.17. Thus, wormlike micelles are formed in solutions at X_1 > 0.17, which is consistent with the decrease of *r*-value. This is also substantiated by the results of DLS measurements and by the TEM pictures as discussed below. It should be pointed out that the inflection point of the η vs X_1 plot exactly matches with the maximum of the *r* vs X_1 plot since vesicle formation does not significantly change the bulk viscosity of the mixtures. The drop of viscosity in mixtures at X_1 > 0.50 can be attributed to transformation of wormlike micelles to spherical micelles. This is shown by the size distribution of the aggregates discussed below.

Figure 4 exhibits size distribution histograms of the aggregates formed in 3 mM C_{12}Gly/SDS mixture of varying composition. Bimodal distribution is observed in solutions at X_1 = 0.05, indicating existence of more than one type of aggregates. Smaller aggregates with mean hydrodynamic diameters of ∼4 nm must be due to spherical micelles which are in equilibrium with large aggregates having mean hydrodynamic diameter at around 100 nm. The large aggregates could be due either to vesicles or to wormlike micelles. Considering the *r*-values of DPH probe in this composition range, the large aggregates can be associated with bilayer vesicles. The low viscosity of the mixtures also supports this conclusion. It is observed that as molar fraction of C_{12}Gly is increased to 0.17 the micellar aggregates gradually disappears with the concomitant formation of vesicles. As seen in Figure 4, in mixtures with 0.17 < X_1 < 0.50, the hydrodynamic diameter of the large aggregates increases with the increase of molar fraction of C_{12}Gly. Interestingly, solutions at X_1 = 0.5 exhibit three size distributions, corresponding to mean hydrodynamic diameters 10, 60, and 350 nm. Since the solution viscosity was also observed to increase in this composition range, it can be concluded that the vesicle structures are transformed into large wormlike micelles, which is consistent with the decrease of *r*-value of DPH probe. Accordingly, the large aggregates having average diameter ∼350 nm must be due to wormlike micelles which is consistent with lower *r*-values of DPH probe in the mixture. The other distributions correspond to rod-like micelles and vesicles that are present in equilibrium with the wormlike micelles. However, it should be noted that DLS technique cannot be applied with the rod-like micelles and therefore, the hydrodynamic sizes of these aggregates mentioned above correspond to equivalent spheres and hence are approximate values only. The size distribution of the aggregates in mixture (3 mM) with X_1 = 0.6 clearly suggests that the large wormlike micelles that exist in mixture at X_1 = 0.5 are transformed into aggregates having shorter relaxation time. This could be either due to formation of smaller mixed micelles with mean hydrodynamic diameter of ca. 5 nm or due to branching of the wormlike micelles. The latter is confirmed by the TEM picture (Figure 5E) as discussed below.

Transmission Electron Microscopy. To visualize the shape (morphology) of the aggregates negatively stained TEM micrographs were obtained for both dilute and concentrated solutions of the surfactant mixture. The micrographs of the aqueous solutions of C_{12}Gly/SDS mixtures at different compositions have been depicted in Figure 5. The TEM images A and B clearly show existence of spherical vesicles in dilute SDS-rich solutions (X_1 = 0.09 and 0.17). The vesicles have inner diameter in the range 75−200 nm. Although shell thickness could not be measured accurately, the vesicles appear to be unilamellar. Recently, others have also reported spontaneous vesicle formation in the binary mixture of an ionic liquid amphiphile and an anionic surfactant (SDS).[39] However, the pictures C and D of the solutions with higher X_1 value (0.5 and 0.6) reveal flexible threads of width equals to twice the length of hydrocarbon chain length. The results are thus consistent with the fluorescence probe and DLS studies described earlier.

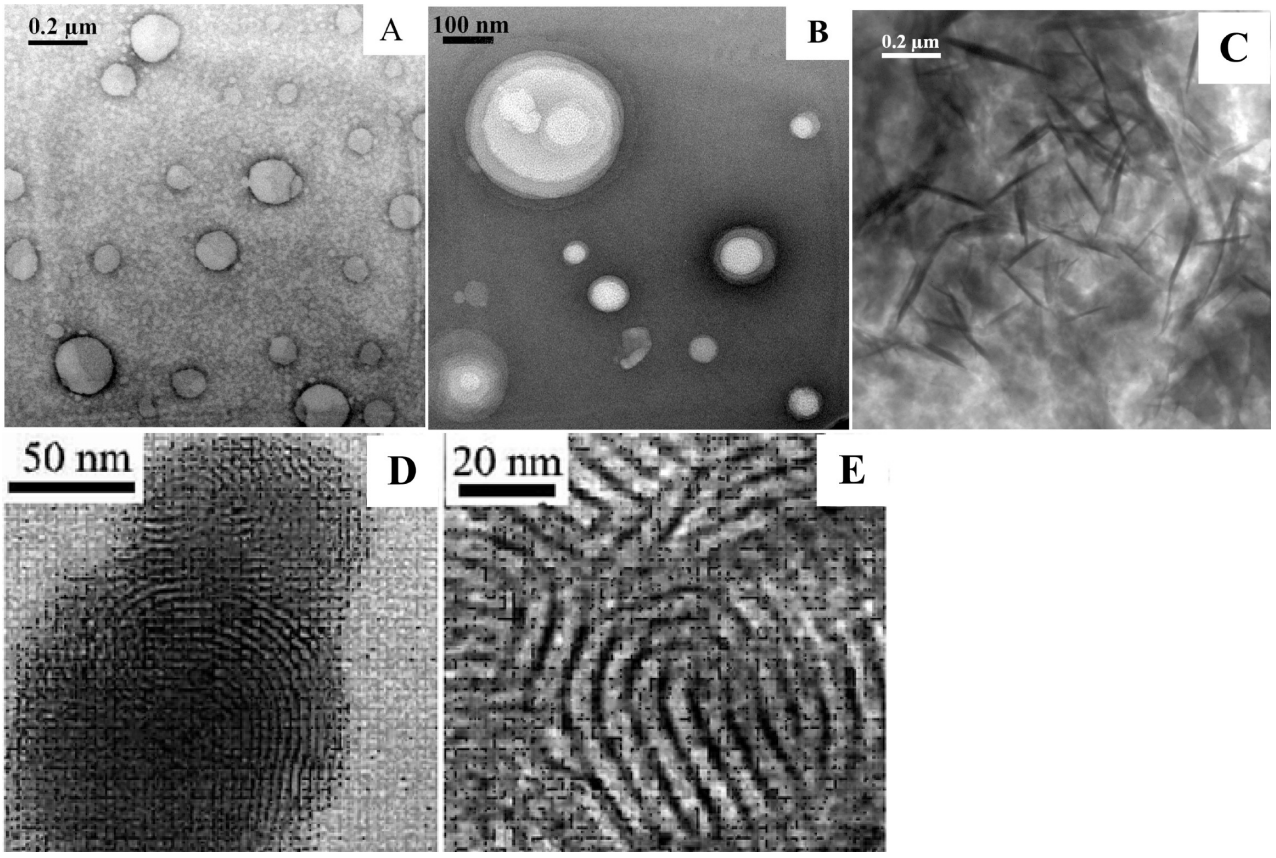

Figure 5. Negatively stained (1% uranyl acetate, pH 7.4) TEM micrographs at different total concentrations of C_{12}Gly/SDS mixtures with different mole fractions (X_1): (A) 0.09 (3 mM), (B) 0.17 (3 mM), (C) 0.17 (30 mM), (D) 0.5 (2 mM), and (E) 0.6 (10 mM).

It is surprising to see that both pictures reveal fingerprint-like texture consisting of flexible threadlike micelles. In contrast to the mixture at $X_1 = 0.50$, the threadlike micelles are observed in concentrated solution at $X_1 = 0.60$. This suggests that threadlike micelles are formed by growth of spherical micelles that exist in dilute solution. The characteristic fingerprint texture is due to lyotropic liquid crystal phase formed in solution. Others have also reported fingerprint-like texture in different surfactant systems.[40] Earlier, we have also reported formation of cholesteric liquid crystal structures in solutions of C_{12}Ala/SDS mixture.[26] The TEM micrograph of C_{12}Ala/SDS system revealed concentric layers of threadlike micelles. The cholesteric behavior of lyotropic liquid crystal systems was explained as due to the presence of chiral centers in the micelle, which induces distortion in the micelle to give a chiral shape. Interactions between chiral micelles then lead to cholesteric behavior.[8,9] Since one of the constituent molecules is chiral, an asymmetry in the interactive forces is obtained. Consequently, information concerning chirality is transmitted via the intermolecular forces and the preferred direction of orientation undergoes a spontaneous twist resulting in the characteristic fingerprint pattern seen under the microscope. However, unlike C_{12}Ala/SDS system, the fingerprint-like texture observed with C_{12}Gly/SDS system does not show concentric circles of threadlike micelles. Therefore, such liquid crystal structures cannot be called as cholesteric phase. This is because in C_{12}Gly/SDS system, there is no chiral center in the C_{12}Gly molecule. This observation therefore supports the mechanism proposed for the generation of cholesteric behavior of lyotropic liquid crystal systems. The threadlike micelles in the case of the C_{12}Gly/SDS system are, however, highly ordered. The average distance between two adjacent threads is about 7 nm. The length of the threadlike micelles could not be precisely measured, but the width of the micelles is about 5 nm. Since the effective hydrocarbon chain length of C_{12}Gly is about 2.09 nm (obtained after energy minimization of the molecular structure by use of MM2 force field using Chem Draw 6.0 software), the threadlike micelles are produced through one-dimensional growth of rod-like micelles.

Fluorescence Microscopy. It is a frequent criticism that negatively stained TEM micrographs result in artifacts because the sample preparation method involves drying of the specimen. Therefore, to substantiate the results obtained from TEM studies we have taken fluorescence microscopic pictures of the mixtures in dilute solutions containing 10 mol % of cholesterol (Chol), which is known to stabilize bilayer membranes. This as well as factors, such as temperature and salt concentration, that influence vesicle stability are discussed in the Supporting Information. The microscopic images have been shown in Figure 6. The pictures of the C_{12}Gly/SDS mixtures clearly reveal the existence of large aggregates with an aqueous dye (CF) entrapped core that resemble vesicular structures. It is interesting to note that the dye entrapped vesicles formed by the C_{12}Gly/SDS mixtures are ~50−250 nm in diameter and are consistent with the results obtained from DLS measurements. This confirms the morphology of the vesicles obtained by TEM or DLS techniques. The interesting phenomenon is that these dye-filled vesicles are not

dx.doi.org/10.1021/la1040147 |*Langmuir* 2011, 27, 5184–5192

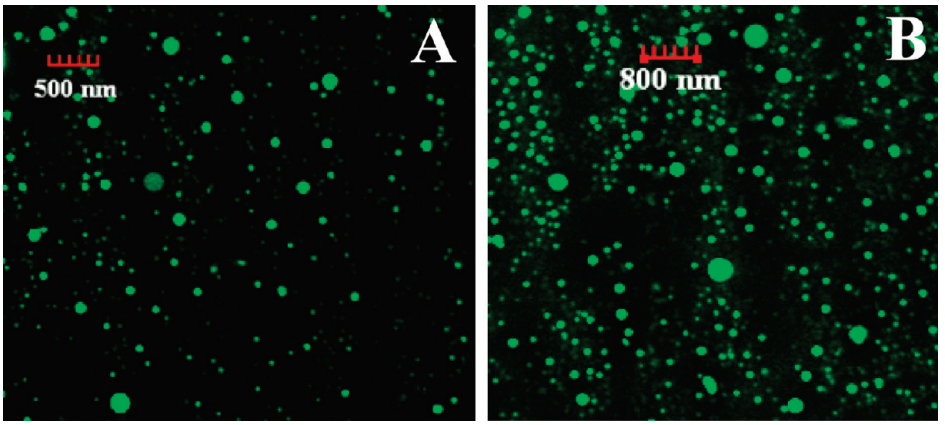

Figure 6. Fluorescence microscopic images of different C_{12}Gly/SDS mixtures (3 mM) containing 10 mol % Chol and 150 mM NaCl in phosphate buffer, pH 7.4: (A) X_1 = 0.09 and (B) X_1 = 0.17 (2 mM).

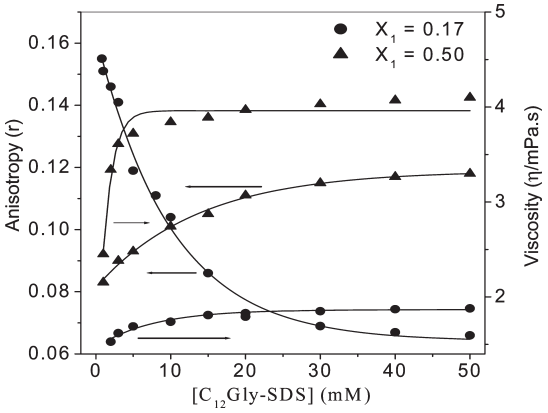

Figure 7. Variation of fluorescence anisotropy (r) of DPH probe and solution viscosity (η) of the binary mixtures in pH 7.4 at X_1 = 0.17 and 0.50 as a function of [C_{12}Gly-SDS].

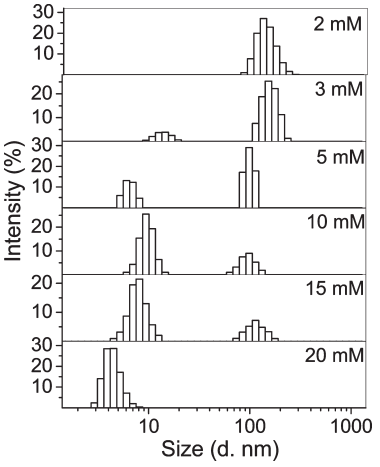

Figure 8. Size distribution histograms of the aggregates at different concentrations of the C_{12}Gly/SDS mixtures (X_1 = 0.17) at 30 °C.

deformed in a way that is usually observed in aggregates. However, we failed to see any aggregates at higher concentrations of the mixtures with X_1 = 0.5. This is because the diameter of the threadlike micelles is around 5 nm which is much less than the resolution of the microscope used.

Effect of Concentration. The shape and size of the aggregates also depend upon the total surfactant concentration. To study the concentration-dependent phase change we have measured r-value of DPH probe at different concentrations of the C_{12}Gly/SDS mixture at X_1 = 0.17. It is interesting to note that at pH 7.4, the r-value decreases with the increase of total surfactant concentration as shown by the plots in Figure 7. This means that hydrocarbon chain packing of the bilayer aggregates formed in dilute solution becomes loosened upon increase of total concentration. This is possible only when the bilayer aggregates are transformed either into spherical micelles or into rod-like micelles; in which the hydrocarbon chains are more fluid compared to bilayer aggregates.[37] The vesicle-to-micelle transition is induced by the increase of total concentration of the mixture and has been reported for many surfactant systems.[41]

The vesicle-to-micelle transition is also supported by the results of DLS measurements. Figure 8 shows the size distributions at various concentrations of the mixture having X_1 = 0.17. It can be observed that the vesicle phase gradually disappears and smaller aggregates with hydrodynamic diameter around 3−5 nm are formed as the total concentration is increased to 20 mM. This is consistent with the decrease of r-value of DPH (Figure 7) probe upon increase of total concentration. However, it should be noted that DLS cannot distinguish shapes of scattering aggregates. Since the solution viscosity (Figure 7) increased with the increase of total concentration of the mixture, the decrease of r-value must be due to the formation of rod-like micelles. This is further confirmed by the TEM picture (Figure 5C) which shows existence of small rod-like micelles of length and diameter of ca.200 and 20 nm, respectively. This means that the vesicle phase exists only in dilute solution of the binary mixture in a narrow range of compositions (X_1 < 0.17) and concentrations (<5 mM), but the vesicles are transformed into rod-like micelles at concentration above 5 mM.

In contrast to the behavior of the binary mixture at X_1 = 0.17, mixtures at X_1 = 0.50 exhibit a small increase of r-value of DPH with the increase of concentration (Figure 7) which reaches plateau at around 50 mM. This is obviously due to the increase of the number of amino acid headgroup at the micelle surface, which causes growth of the wormlike micelles forming threadlike micelles. The one-dimensional growth of micelles should increase rigidity of the hydrocarbon chains. Formation of threadlike micelles

dx.doi.org/10.1021/la1040147 |*Langmuir* 2011, 27, 5184–5192

is normally manifested by the increase of bulk viscosity of water. Indeed, during sample preparation, it was observed that bulk viscosity of water increased upon increase of total concentration of the mixture. The viscosity change of the binary mixture at X_1 = 0.50 was therefore systematically studied at different concentrations. The data are presented by the plot in Figure 7, which exhibits gradual increase of viscosity with the increase of concentration reaching plateau at a total concentration equal to 50 mM. It is well-known that enhancement of bulk viscosity is proportional to the size of the rod-like micelles.[42] Thus, the increase of viscosity of a surfactant solution can be attributed to the formation of threadlike micelles. Surfactant solutions containing long threadlike micelles have higher viscosity because of entanglement of the micelles. Despite the high aspect ratio of the threadlike micelles (see Figure 5), the apparent viscosity of the isotropic solution of the C_{12}Gly/SDS system is not very high. This is because the threads are found to be connected with others at places. The lower solution viscosity as a result of branching of the rod-like micelles has also been reported by others.[43] In fact, micellar branching in solutions of nonionic,[44] ionic,[43] and mixed surfactant systems[45] is well-known. Porte et al. first suggested the occurrence of micellar branching.[46] It has been suggested that entropic factor is responsible for micellar defects, such as "end-caps" or "Y-junctions".[47]

4. CONCLUSIONS

In summary, we have studied interactions between zwitterionic (C_{12}Gly) and anionic (SDS) surfactants. The mixed C_{12}Gly/SDS systems were observed to have much lower cmc and have greater surface activity not only compared to individual surfactants, but also compared to other surfactants and surfactant mixtures reported in the literature. The synergism is due to nonideal mixing and strong electrostatic interaction (as indicated by the negative β values) between C_{12}Gly and SDS surfactants to form a pseudodouble chain anionic surfactant. The composition dependence of β values has indicated formation of aggregates of different shapes. In dilute solutions (<3 mM) with mixing ratios $X_1 \leq 0.17$, the mixed system exhibit vesicle formation, which is favored more in alkaline pH. In acidic pH, the vesicles are converted to small mixed micelles. This suggests that the vesicles thus prepared may find applications in pH-induced controlled drug release. The mixed system with X_1 = 0.17 also exhibit vesicle-to-micelle (rod-like) transition upon increase of total concentration. However, only long threadlike micelles were observed in concentrated solutions of the mixtures with $X_1 >$ 0.17. It is interesting to note that the binary mixtures containing higher molar fractions of C_{12}Gly (X_1 = 0.5 and 0.6) exhibit fingerprint-like structures showing branching of the flexible threadlike micelles.

■ ASSOCIATED CONTENT

Supporting Information. Surface tension plots, detailed studies on the effect of salt on solution viscosity, and stability of vesicles as a function of pH, temperature, salt and cholesterol concentration have been presented. This material is available free of charge via the Internet at http://pubs.acs.org.

■ AUTHOR INFORMATION

Corresponding Author

*Phone: 91-3222-283308. Fax: 91-3222-255303. E-mail: joydey@chem.iitkgp.ernet.in.

■ ACKNOWLEDGMENT

Authors gratefully acknowledge Department of Science and Technology, New Delhi, for financial assistance (Grant No. SR/S1/PC-18/2005) of this work. The authors are thankful to Dr. N. Sarkar for the DLS measurements.

■ REFERENCES

(1) (a) Moulik, S. P.; Haque, M. E.; Jana, P. K.; Das, A. R. *J. Phys. Chem.* **1996**, *100*, 701–708. (b) Haque, M. E.; Das, A. R.; Moulik, S. P. *J. Phys. Chem.* **1995**, *99*, 14032–14038.

(2) Sharma, K. S.; Patil, S. R.; Rakshit, A. K. *J. Phys. Chem. B* **2004**, *108*, 12804–12812.

(3) Jana, P. K.; Moulik, S. P. *J. Phys. Chem.* **1991**, *95*, 9525–9532.

(4) Haque, M. E.; Das, A. R.; Rakshit, A. K.; Moulik, S. P. *Langmuir* **1996**, *12*, 4084–4089.

(5) Sulthana, S. B.; Rao, P. V. C.; Bhat, S. G. T.; Nakano, T. Y.; Sugihara, G.; Rakshit, A. K. *Langmuir* **2000**, *16*, 980–987.

(6) Castaldi, M. L.; Ortona, O.; Paduano, L.; Vitagliano, V. *Langmuir* **1998**, *14*, 5994–5998.

(7) Sulthana, S. B.; Rao, P. V. C.; Bhat, S. G. T.; Rakshit, A. K. *J. Phys. Chem. B* **1998**, *102*, 9653–9660.

(8) Bury, R.; Treiner, C.; Chevalet, J.; Makayssi, A. *Anal. Chim. Acta* **1991**, *251*, 69–77.

(9) Makayssi, A.; Bury, R.; Treiner, C. *Langmuir* **1994**, *10*, 1359–1365.

(10) Jacobson, A. M.; Crars, F. *J. Colloid Interface Sci.* **1991**, *142*, 480–488.

(11) Kaler, E. W.; Murthy, A. K.; Rodriguez, B. E.; Zasadzinski, J. A. *Science* **1989**, *245*, 1371–1374.

(12) Shioi, A.; Hatton, T. A. *Langmuir* **2002**, *18*, 7341–7348.

(13) (a) Marques, E. F.; Brito, R. O.; Silava, S. G.; Rodríguez-Borges, J. E.; do Vale, M. L.; Gomes, P.; Araújo, M. J.; Soderman, O. *Langmuir* **2008**, *24*, 11009–11017. (b) Silva, B. F. B.; Marques, E. F.; Olsson, U. *Langmuir* **2008**, *24*, 10746–10754.

(14) (a) Brito, R. O.; Marques, E. F.; Gomes, P.; Falcao, S.; Söderman, O. *J. Phys. Chem. B* **2006**, *110*, 18158–18165. (b) Shrestha, R. G.; Shrestha, L. K.; Aramaki, K. *J. Colloid Interface Sci.* **2007**, *311*, 276–284.

(15) Rosa, M.; Miguel, MdaG.; Lindman, B. *J. Colloid Interface Sci.* **2007**, *312*, 87–97.

(16) Jung, H. T.; Coldren, B.; Zasadzinski, J. A.; Iampietro, D. J.; Kaler, E. W. *P. Natl. Acad. Sci. U.S.A.* **2001**, *98*, 1353–1357.

(17) (a) Khan, A.; Marques, E. F. *Curr. Opin. Colloid Interface Sci.* **2000**, *4*, 402–410. (b) Kume, G.; Gallotti, M.; Nunes, G. *J. Surfact. Deterg.* **2008**, *11*, 1–11.

(18) (a) Christov, N. C.; Denkov, N. D.; Kralchevsky, P. A.; Ananthapadmanabhan, K. P.; Lips, A. *Langmuir* **2004**, *20*, 565–571. (b) Rosen, M. J. *Langmiur* **1991**, *7*, 885–888. (c) Iwasaki, T.; Ogawa, M.; Esumi, K.; Meguro, K. *Langmuir* **1991**, *7*, 30–35. (d) Li, F.; Li, G. Z.; Chen, J. B. *Colloids Surf. A* **1998**, *145*, 167–174. (e) López-Díaz, D.; García-Mateos, I.; Velázquez, M. M. *Colloids Surf. A* **2005**, *270−271*, 153–162.

(19) McLachlan, A. A.; Marangoni, D. G. *J. Colloid Interface Sci.* **2006**, *295*, 243–248.

(20) Li, F.; Li, G.-Z.; Chen, J.-B. *Colloids Surf. A* **1998**, *145*, 167–174.

(21) Hoffmann, H.; Gräbner, D.; Hornfeck, U.; Platz, G. *J. Phys. Chem. B* **1999**, *103*, 611–614.

(22) Weiss, T. M.; Narayanan, T.; Gradzielski, M. *Langmuir* **2008**, *24*, 3759–3766.

(23) Christov, N. C.; Denkov, N. D.; Kralchevsky, P. A.; Anantha-padmanabhan, K. P.; Lips, A. *Langmuir* **2004**, *20*, 565–571.

(24) (a) Du, N.; Song, S.-E.; Hou, W.-G. *Colloids Surf. A* **2008**, *312*, 104–112. (b) Rosa, M.; Infantc, M. R.; Miguel, M; da., G.; Lindman, B. *Langmuir* **2006**, *22*, 5588–5596. (c) Zhai, L. M.; Zhang, J. Y.; Shi, Q.-X.; Chen, W. J.; Zhao, M. *J. Colloid Interface Sci.* **2005**, *284*, 698–703.

(25) Wolf, C.; Bressel, K.; Drechsler, M.; Gradzielski, M. *Langmuir* **2009**, *25*, 11358–11366.
(26) Khatua, D.; Ghosh, S.; Dey, J.; Ghosh, G.; Aswal, V. K. *J. Phys. Chem. B* **2008**, *112*, 5374–5380.
(27) Khatua, D.; Dey, J. *Langmuir* **2005**, *21*, 109–114.
(28) Khatua, D.; Maiti, R.; Dey, J. *J. Chem. Soc. Chem. Commun.* **2006**, 4903–4905.
(29) Mata, J.; Varade, D.; Ghosh, G.; Bahadur, P. *Colloids Surf. A* **2004**, *245*, 69–73.
(30) Pecora, R., Ed. *Dynamic Light Scattering: Applications of Photon Correlation Spectroscopy*; Plenum Press: New York, London, 1985.
(31) Rubingh, D. N. In *Solution Chemistry of Surfactants*: Mittal, K. L., Ed.; Plenum Press: New York, 1979; Vol. 1, pp 337−354.
(32) Rosen, M. J. *Surfactants and Interfacial Phenomena*, 4th ed.; John-Wiley: New York, 2004.
(33) Rosen, M. J.; Hua, X. Y. *J. Colloid Interface Sci.* **1982**, *86*, 164–172.
(34) (a) Misselyn-Bauduin, A. M.; Thibaut, A.; Grandjean, J.; Broze, G.; Jerome, R. *Langmuir* **2000**, *16*, 4430–4435. (b) López-Díaz, D.; García-Mateos, I.; Velázquez, M. M. *Colloids Surf. A* **2005**, *270−271*, 153–162. (c) Wang, Z.-Y.; Zhang, S.-F.; Fang, Y.; Qi, L.-Y. *J Surfact. Deterg.* **2010**, *13*, 381–385.
(35) (a) Motomura, K.; Iwanaga, S.; Yamanaka, M.; Aratono, M.; Matuura, R. *J. Colloid Interface Sci.* **1982**, *86*, 151–157. (b) Yamanaka, M.; Iyota, H.; Aratono, M.; Motomura, K.; Matuura, R. *J. Colloid Interface Sci.* **1983**, *94*, 451–455. (c) Motomura, K.; Iwanaga, S.; Uryu, S.; Matsukiyo, H.; Yamanaka, M.; Matuura, R. *Colloids Surf.* **1984**, *9*, 19–31. (d) Yamanaka, M.; Aratono, M.; Motomura, K.; Matuura, R. *Colloid Polym. Sci.* **1984**, *262*, 338–341.
(36) (a) Moroi, Y.; Nishikido, N.; Matuura, R. *J. Colloid Interface Sci.* **1975**, *50*, 344–351. (b) Motomura, K.; Yamanaka, M.; Aratono, M. *Colloid Polym. Sci.* **1984**, *262*, 948–955.
(37) Roy, S.; Mohanty, A.; Dey, J. *Chem. Phys. Lett.* **2005**, *414*, 23–27.
(38) Shinitzky, M. In *Physical Methods on Biological Membranes and Their Model Systems*; Plenum Publishing Corp.: New York, 1984; p 237.
(39) (a) Yuan, J.; Bai, X.; Zhao, M.; Zheng, L. *Langmuir* **2010**, *26*, 11726–11731. (b) Singh, K.; Marangoni, G. M.; Quinn, J. G.; Singer, R. D. *J. Colloid Interface Sci.* **2009**, *335*, 105–111. (c) Zhai, L.; Zhao, J.; Zhao, M.; Chen, Y.; Zhang, L. *J. Disp. Sci. Technol.* **2007**, *28*, 455–461.
(40) (a) Nieh, M.-P.; Harroun, T. A.; Raghunathan, V. A.; Glinka, C. J.; Katsaras, J. *Biophys. J.* **2004**, *86*, 2615–2629. (b) Yu, L. J.; Saupe, A. *J. Am. Chem. Soc.* **1980**, *102*, 4879–4883.
(41) (a) Mohanty, A.; Patra, T.; Dey, J. *J. Phys. Chem. B* **2007**, *111*, 7155–7159. (b) Yan, Y.; Hoffmann, H.; Drechsler, M.; Talmon, Y.; Makarsky, E. *J. Phys. Chem. B* **2006**, *110*, 5621–5626. (c) Feitosa, E.; Bonassi, N. M.; Loh, W. *Langmuir* **2006**, *22*, 4512–4517. (d) Davies, T. S.; Ketner, A. M.; Raghavan, S. R. *J. Am. Chem. Soc.* **2006**, *128*, 6669–6675. (e) Johnsson, M.; Wagenaar, A.; Engberts, J. B. F. N. *J. Am. Chem. Soc.* **2003**, *125*, 757–760.
(42) (a) Kalur, G. C.; Frounfelker, D.; Cipriano, B. H.; Norman, A. I.; Raghavan, S. R. *Langmuir* **2005**, *21*, 10998–11004. (b) Angelescu, D.; Khan, A.; Caldararu, H. *Langmuir* **2003**, *19*, 9155–9161.
(43) (a) Gonzalez, Y. I.; Kaler, E. W. *Curr. Opin. Colloid Interface Sci.* **2005**, *10*, 256–260. (b) Shashkina, J. A.; Philoppova, O. E.; Zaroslov, Y. D.; Khokhlov, A. R.; Pryikhina, T. A.; Blagodatskikh, I. V. *Langmuir* **2005**, *21*, 1524–1530. (c) Flood, C.; Dreiss, C. A.; Croce, V.; Cosgrove, T.; Karlsson, G. *Langmuir* **2005**, *21*, 7646–7652. (d) Schubert, B. A.; Kaler, E. W.; Wagner, N. J. *Langmuir* **2003**, *19*, 4079–4089. (e) Raghavan, S. R.; Edlund, H.; Kaler, E. W. *Langmuir* **2002**, *18*, 1056–1064. (f) Bernheim-Groswasser, A.; Zana, R.; Talmon, Y. *J. Phys. Chem. B* **2000**, *104*, 4005–4009.
(44) Bernheim-Groswasser, A.; Watchtel, E.; Talmon, Y. *Langmuir* **2000**, *16*, 4131–4140.
(45) (a) Bernheim-Groswasser, A.; Zana, R.; Talmon, Y. *J. Phys. Chem. B* **2000**, *104*, 12192–12201. (b) Koehler, R. D.; Raghavan, S. R.; Kaler, E. W. *J. Phys. Chem. B* **2000**, *104*, 11035–11044. (c) Kwon, S. Y.; Kim, M. W. *Phys. Rev. Lett.* **2002**, *89*, 258302–258304. (d) Ghosh, A.; Dey, J. *Langmuir* **2008**, *24*, 6018–6026. (e) Ghosh, A.; Dey, J. *J. Phys. Chem. B* **2008**, *112*, 6629–6635.
(46) Porte, G.; Gomati, R.; Haitami, O. E.; Appell, J.; Marignan, J. *J. Phys. Chem.* **1986**, *90*, 5746–5751.
(47) Israelachvili, J. N. *Intermolecular and Surface Forces*, 2nd ed.; Academic Press: New York, 1991.